

# Enhanced efficacy of AZD3759 and radiation on brain metastasis from EGFR mutant non-small cell lung cancer

Xue Li<sup>1,2</sup>, Yingchun Wang<sup>3</sup>, Jia Wang<sup>3</sup>, Tianwei Zhang<sup>3</sup>, Li Zheng<sup>3</sup>, Zhenfan Yang<sup>3</sup>, Ligang Xing<sup>2</sup> and Jinming Yu <sup>2</sup>

<sup>1</sup> Department of Radiation Oncology and Key Laboratory of Cancer Prevention and Therapy, Tianjin Medical University Cancer Institute and Hospital, National Clinical Research Center for Cancer, Tianjin 300060, China

<sup>2</sup> Department of Radiation Oncology, Shandong Cancer Hospital Affiliated to Shandong University, Shandong Academic of Medical Science, Jinan 250117, China

<sup>3</sup> Asia Innovative Medicines and Early Development, AstraZeneca, Shanghai 201203, China

The prognosis of patients with brain metastasis (BM) is poor. In our study, we demonstrated that AZD3759, an EGFR tyrosine kinase inhibitors (TKIs) with excellent blood–brain barrier (BBB) penetration, combined with radiation enhanced the antitumor efficacy in BM model from EGFR mutant (EGFRm) NSCLC. Besides, the antitumor activity displayed no difference between radiation concurrently with AZD3759 and radiation sequentially with AZD3759. Mechanistically, we found that two factors determined the enhanced efficacy: cells with EGFRm which were sensitive to AZD3759, and a relative high concentration of AZD3759. We have validated mechanisms underlying the radiosensitizing effect of AZD3759, which were involved in decreased cell proliferation and survival, and suppressed repair of DNA damage. Moreover, our study found that AZD3759 inhibited both the non-homologous end joining (NHEJ) and homologous recombination (HR) DNA double-strand breaks (DSBs) repair pathway, and abrogated the G2/M checkpoint to suppress DNA damage repair. We also detected the BBB penetration of AZD3759 when combined with cranial radiation. The results showed the BBB penetration of AZD3759 was decreased within 24 hr after radiation, however, the free concentration of AZD3759 in brain kept at a high level in the context of radiation. In conclusion, our findings suggest that AZD3759 combined with radiation enhances the antitumor activity in BM from EGFRm NSCLC, this combination therapy may be an effective treatment option for BM from EGFRm NSCLC.

## Introduction

About 25–50% of patients with non-small cell lung cancer (NSCLC) will develop brain metastasis (BM) during their disease course,<sup>1</sup> and the incidence is even higher in patients harboring epidermal growth factor receptor activating mutations (EGFRm).<sup>2,3</sup> BM from NSCLC is associated with poor prognosis, with a median overall survival (OS) of 3–15 months depending on the prognostic factors.<sup>4,5</sup>

Treatment options for BM include resection or stereotactic radiosurgery (SRS) with or without whole-brain radiotherapy (WBRT) for patients with a limited number of BM.<sup>6</sup> WBRT was considered as the standard of care in patients not suitable for local treatments. EGFR tyrosine kinase inhibitors (TKIs), such as gefitinib and erlotinib, have displayed some benefits in BM from EGFRm NSCLC, while variation in progression free survival (PFS) was reported in these studies,

**Key words:** AZD3759, radiation, brain metastasis, non-small cell lung cancer, epidermal growth factor receptor

**Abbreviation:** AUC: area under the concentration time curve; BBB: blood–brain barrier; BM: brain metastasis; CC3: cleaved caspase 3; CFA: cloning formatting assay; CNS: central nervous system; co-IP: coimmunoprecipitation; C<sub>t</sub>(blood): total concentration of AZD3759 in blood; C<sub>t</sub>(brain): total concentration of AZD3759 in brain; C<sub>u</sub>(blood): unbound concentration of AZD3759 in blood; C<sub>u</sub>(brain): unbound concentration of AZD3759 in brain; DEF: dose enhancement factors; DSBs: double-strand breaks; EGFRm: epidermal growth factor receptor activating mutations; GAPDH: glyceraldehyde-3-phosphatedehydrogenase; IF: immunofluorescence; IHC: immunohistochemistry; NBF: neutral buffered formalin; NSCLC: non-small cell lung cancer; OS: overall survival; PFS: progression free survival; SRS: stereotactic radiosurgery; TKIs: tyrosine kinase inhibitors; WBRT: whole-brain radiotherapy; WT: wild type

Additional Supporting Information may be found in the online version of this article.

**Grant sponsor:** National Natural Science Foundation of China; **Grant number:** 81472812; **Grant sponsor:** Innovation Project of Shandong Academy of Medical Science; **Grant sponsor:** National Health and Family Planning Commission of China; **Grant number:** 201402011

**DOI:** 10.1002/ijc.31303

**History:** Received 30 Sep 2017; Accepted 2 Feb 2018; Online 12 Feb 2018

**Correspondence to:** Ligang Xing, Department of Radiation Oncology, Shandong Cancer Hospital Affiliated to Shandong University, Shandong Academic of Medical Science, 440 Jiyan Road, Jinan, Shandong, China, Tel.: 86-531-67626819, Fax: 86-531-67626819, E-mail: xinglg@medmail.com.cn; or Jinming Yu, Department of Radiation Oncology, Shandong Cancer Hospital Affiliated to Shandong University, Shandong Academic of Medical Science, 440 Jiyan Road, Jinan, Shandong, China, Tel.: 86-531-87984729, Fax: 86-531-87984729, E-mail: sdyujinming@163.com

**What's new?**

Epidermal growth factor receptor (EGFR)-tyrosine kinase inhibitors (TKIs) have shown a radiosensitizing effect in extracranial tumors, suggesting the potential of combining a blood-brain barrier penetrating agent with radiation as a new therapeutic approach to brain metastasis. This study shows that AZD3759, an EGFR-TKI with excellent blood-brain barrier penetration, combined with radiation enhances antitumor efficacy on brain metastasis from EGFR mutant non-small cell lung cancer (NSCLC) sensitive to AZD3759. AZD3759 with sequential or concurrent radiation achieved comparable efficacy. The results warrant further clinical studies to investigate AZD3759 combined with radiation as a potentially effective treatment for brain metastasis in EGFRm NSCLC.

probably due to small sample size.<sup>7,8</sup> Besides, several clinical studies have been conducted to evaluate the role of EGFR-TKIs combined with radiation in the treatment of BM from NSCLC.<sup>9–11</sup> However, the results from two phase III studies showed that combination therapy with radiation and erlotinib did not further improve patients survival compared to radiation alone.<sup>9,11</sup> Possible explanations include these studies were conducted in NSCLC patients with unselected EGFR mutation status, and limited blood-brain barrier (BBB) penetration of gefitinib and erlotinib led to insufficient drug concentration in the brain for target inhibition.

In contrast to the negative clinical results in BM, radiosensitizing effect of EGFR-TKIs was reported in extracranial tumors in both clinical and preclinical settings,<sup>12–16</sup> suggesting the potential of combining a BBB-penetrating agent with radiation for BM. AZD3759 was an EGFR-TKIs with good BBB penetration in both preclinical and clinical settings, and showed promising activity in patients with central nervous system (CNS) metastasis as monotherapy.<sup>17,18</sup> In our study, we evaluated the potential of AZD3759 in combination with radiation in a BM model in mice, and explored the mechanism underneath. The result of our study provides preclinical evidence for further development of AZD3759.

**Materials and Methods****Cell line and reagents**

The human NSCLC cell lines NCI-H3255 (H3255, EGFR L858R), NCI-H226 (H226, EGFR wild type) and NCI-H2228 (H2228, EGFR wild type) were purchased from the American Type Culture Collection. The PC-9 (Exon19del) cell line was obtained in 2011 from A. Hiraide at Preclinical Sciences R&D, AstraZeneca, Osaka, Japan. All cell lines were authenticated by short-tandem repeat analysis within 6 months of performing the experiments.

PC-9 cells transfected with pGL4.50[luc2/CMV/Hygro] vector containing luciferase (PC-9\_Luc cell) were used for establishing brain metastasis model *in vivo*. The stable cell clone was selected with hygromycin B (300 mg/mL) by serial dilution, and the bioluminescence signal was measured by a Xenogen imaging system (Xenogen IVIS 200).

AZD3759 was provided by AstraZeneca (Shanghai, China), and was dissolved in dimethyl sulfoxide (Sigma, St.

Louis, MO, USA) in *in vitro* study. In *in vivo* study, the formulation for the drug was 1% methyl cellulose (Sigma; 9004-67-5) in water.

**Cell growth inhibition**

The effect of AZD3759 and radiation on cell proliferation was evaluated using MTS assay (tetrazolium-based CellTiter 96 Aqueous One Solution Proliferation assay, Promega, Madison, WI, USA, G3581) as described previously.<sup>19</sup> Briefly, exponentially growing cells were diluted to desired cell density and seeded 100  $\mu$ L/well into 96-well plates (Corning, Corning, NY, USA). Twenty-four hours later, cells were treated with radiation and increasing concentrations of AZD3759, AZD3759 was dosed 1 hr prior radiation. Then, MTS assay was performed 3 days later. Relative cell viability was expressed as the percentage of untreated control. The Chou-Talalay median effect analysis was performed to determine whether there was synergistic effect between radiation and AZD3759. The combination index (CI) was calculated using CompuSyn software.<sup>20</sup> A CI value <1, =1 and >1 indicates synergistic, additive and antagonistic effects, respectively. Experiments were repeated three independent times.

**Clonogenic assay**

Survival after treatment with radiation and AZD3759 was assessed using cloning formatting assay (CFA) as described before.<sup>21</sup> Dose enhancement factors (DEF) was calculated as the ratio of the radiation dose that produced 10% cell survival on the radiation-only survival curve divided by that for the corresponding radiation combined with AZD3759 survival curve. A value of DEF >1 indicates radiosensitization. Experiments were repeated three independent times.

**Immunofluorescence (IF)**

The DNA double-strand breaks (DSBs) was assessed by measuring the mean percentage of cells with positive  $\gamma$ H2AX ( $\geq 5$  foci per cell) using immunofluorescence (IF) assay as described before.<sup>22,23</sup> Briefly, exponentially growing PC-9 cells were plated at 30–40% confluence in chamber slides (Thermo, Waltham, MA, USA, 154534). At the specified time points after different treatments, cells were fixed (4% formaldehyde, 15 min at room temperature) and blocked (5% bovine serum albumin in PBS for 1 hr), then incubated with

anti-phospho-histone H2AX (Ser139) (CST, 2577S; 1:800 dilution) overnight at 4°C. After washed in PBS (3 times), cells were incubated in Alexa 488-conjugated anti-rabbit secondary antibody (CST, 4412S; 1:1,000 dilution) for 1 hr at room temperature in the dark. Following PBS washing (3 times), the slides were mounted with Prolong Gold Antifade Reagent with DAPI. Images were acquired with Olympus BX61 microscope with 60× objective. For quantitative analysis, nuclei were analyzed by eye. At least 150 cells for each condition were randomly selected to determine the percentage of cells as “positive” for  $\gamma$ H2AX ( $\geq 5$  foci per cell). Experiments were repeated three independent times.

#### Flow cytometry

At the specified time points after different treatments, cells were trypsinized and washed with ice-cold PBS. For cell cycle analysis, cells were fixed in ice-cold 70% ethanol and stored at 4°C overnight. After removal of ethanol by centrifugation, cells were incubated with a solution of 0.05 mg/mL propidium iodide (PI) and 0.2 mg/mL RNase A in the dark at room temperature for 20–30 min. Samples were then analyzed using a Becton Dickinson FACScan flow cytometer. Resulting DNA distributions were analyzed by Modfit (Verity Software House, Inc., Topsham, ME) for the proportion of cells in sub-G1, G1, S and G2/M phases. Experiments were repeated three independent times.

#### Coimmunoprecipitation and western blot

Exponentially growing PC-9 cells were plated at 70–80% confluence. Twenty-four hours later, cells were treated as described and harvested at the specified time points. Cytoplasmic and nuclear extraction were prepared according to the instructions of the NE-PER Nuclear and Cytoplasmic Extraction Reagents (Thermo 78835). Coimmunoprecipitation (co-IP) was performed according to the instructions of the Pierce™ Classic Magnetic IP/Co-IP Kit (Thermo 88804). Briefly, EGFR was immunoprecipitated from 500  $\mu$ g of cell lysate with 1  $\mu$ g IgG goat anti-hEGFR antibody (R&D, AF231), over night at 4°C. Western blot analysis was performed according to the standard procedures with 20  $\mu$ g cell lysate. The primary antibodies were diluted as follows: EGFR (CST, 4267S) 1:1,000, phospho-EGFR (Y1068) (CST, 2234S) 1:1,000, DNA-PKcs (Santa Cruz, D2914) 1:1,000, AKT (CST, 4685S) 1:1,000, phospho-AKT (S473) (CST, 9271S) 1:1,000, p38/40 MAPK (ERK1/2) (CST, 4695S) 1:1,000, pERK1/2 T202/Y204 (CST, 4370S) 1:1,000, PARP (CST, 9532S) 1:1,000, caspase 3 (CST, 9662S) 1:1,000, rad51 (CST, 8875S) 1:1,000, cdc2 (CST, 9116 sec) 1:1,000, phospho-cdc2 (Y15) (CST, 9111S) 1:1,000, GAPDH (CST, 2118L) 1:10,000, lamin B1 (CST, 15068S) 1:1,000. Immunoblots were quantitated with Image-J (NIH).

#### Mice and brain metastasis model

Six- to 8-week-old female Nu/Nu mice were obtained from Vital River and maintained under pathogen-free conditions

in the animal facility at AstraZeneca (Shanghai, China). All animal experiments were approved by the Institutional Animal Care and Use Committee (IACUC) of AstraZeneca. For animal welfare, mice were euthanatized 100 days later after treatment start or when body weight loss  $\geq 20\%$ .

To establish a brain metastasis model, about  $5 \times 10^5$  PC-9\_Luc cells were injected into the brain parenchyma of mice using the method as described before.<sup>24</sup> Approximately 2–3 weeks later when luciferin signals reached  $>5 \times 10^6$  photons/sec, BM bearing mice were randomized into five treatment groups, including (1) vehicle; (2) AZD3759 alone; (3) radiation alone (30 Gy/10 daily fraction, 5 fraction per week); (4) radiation concurrently with AZD3759; (5) radiation sequentially with AZD3759. AZD3759 was administered by oral gavage at 15 mg/kg once daily until the end of the study. Radiation treatment was performed at room temperature at a dose rate of 1.6 Gy/min using a XCELL 160 X-ray system (Kubtec, Stratford, CT, USA). BM bearing mice were immobilized on a jigs and sheltered by a lead to expose only the head to radiation. In the concurrent treatment group, AZD3759 was administered 1 hr prior radiation. In the sequential treatment group, BM bearing mice were treated with radiation firstly, 3 weeks later after treatment start, AZD3759 was administered as described above until the end of the study. Tumor growth was monitored by measuring bioluminescence signals weekly, and body weight change of mice was also measured during the study.

#### Immunohistochemistry (IHC) assay

Brain tissues of tumor-bearing mice were collected at the indicated time points after treatments with a single dose of radiation or radiation combined with AZD3759 15 mg/kg. Then tissues were fixed in 10% neutral buffered formalin (NBF) overnight following standard procedure for processing, paraffin-embedding and sectioning for IHC assay. IHC assay was performed as described previously,<sup>18</sup> and the following antibodies were used: pEGFR (Y1068) (CST, 2234) 1:200, Ki-67 (Dako, Glostrup, Denmark, M7240) 1:300, cleaved caspase 3 (CST, 9661) 1:100. The IHC signals were quantified by the Aperio image analysis system. The pEGFR (Y1068) was expressed as an “H” score, both staining intensity and positive percentage were used to generate the H score. The Ki-67 was expressed as an index as the percentage of positive cells. The cleaved caspase 3 (CC3) was expressed as the percentage of positive cells.

#### H&E assay

To evaluate tumor area at the end of *in vivo* efficacy study, we performed HE assay. Briefly, mice brain were collected when mice were died during study or sacrificed at days 100. Brain tissues were processed as described for IHC assay. Then, we performed serial section to found the maximum cross-section of tumors, and HE assay was performed as described before. The tumor area was quantified by the Aperio image analysis system.

### Mice pharmacokinetic studies

The CNS penetration of AZD3759 was assessed by a single dose absorption assay as described before.<sup>17,18</sup> Briefly, three mice per dose group and time point received a single dose of radiation, AZD3759 15 mg/kg or radiation combined with AZD3759 15 mg/kg. AZD3759 was dosed 1 hr before radiation. Mice were terminated (rising CO<sub>2</sub> dose) and blood and brain samples were collected 2, 4, 8, 16 and 24 hr post AZD3759 dosing. Drug concentrations in the blood and brain were analyzed by LC-MS/MS.

The biologically active unbound concentration of AZD3759 in brain ( $C_u(\text{brain})$ ) and blood ( $C_u(\text{blood})$ ) was calculated as follows:  $C_u(\text{brain}) = C_t(\text{brain}) \times f_{u,\text{brain}}$ ,  $C_u(\text{blood}) = C_t(\text{blood}) \times f_{u,\text{blood}}$ , where  $C_t(\text{brain})$  and  $C_t(\text{blood})$  are the total concentration of AZD3759 in brain and blood, respectively;  $f_{u,\text{brain}}$  and  $f_{u,\text{blood}}$  are the fraction of unbound AZD3759 in brain and blood, respectively.  $f_{u,\text{brain}}$  and  $f_{u,\text{blood}}$  were determined by equilibrium dialysis. Exposure was expressed as area under the plasma or brain-concentration time curve (AUC) from 0 to 24 hr.<sup>25</sup>  $K_{p,\text{brain}}$  is the ratio of total AUC in brain to total AUC in blood, which was used to evaluate the distribution of AZD3759 in brain and blood.  $K_{p_{\text{uu}},\text{brain}}$  is the ratio of unbound AUC in brain to unbound AUC in blood, which was used to evaluate the relative concentration of biologically active AZD3759 in brain and blood.

The activity of AZD3759 in brain was evaluated by detecting the extent and duration of pEGFR reduction relative to the free concentration of AZD3759 in brain.<sup>26</sup>

### Statistical analysis

Data are represented on graphs as the mean  $\pm$  SEM of three independent experiments. *t*-Test was used for the comparison of percentage of  $\gamma$ H2AX positive cells in the IF assay, percentage of cells in G1, S, G2/M phase and percentage of apoptosis in the flow cytometry assay, and the expression of Ki-67 and CC3 in the IHC assay, between cells treated with radiation combined with AZD3759 and cells treated with radiation alone or AZD3759 alone. The two-way ANOVA was applied for the comparison of luciferin signals in the BM models. All the analyses aforementioned were performed using GraphPad Prism software. The clonogenic survival data were fitted by linear regression according to the linear-quadratic equation  $S(D) = \exp(\alpha D + \beta D^2)$ , where  $D$  is the radiation dose,  $S$  is the survival fraction at the radiation dose of  $D$ ,  $\alpha$  is the linear parameter and  $\beta$  is the quadratic parameter.  $\alpha$  and  $\beta$  are calculated from the survival data using the method described by Franken *et al.*<sup>21</sup> Linear regression analyses were performed to determine whether there were synergistic effect between radiation and AZD3759 in CFA, *p*-values of  $<0.05$  indicate synergistic effect. The analysis of clonogenic survival data was performed using SPSS software (IBM). *p*-Values of  $<0.05$  were considered statistically significant.

## Results

### Sensitivity to AZD3759 and concentration of AZD3759 determine the synergistic effect between AZD3759 and radiation

First, we determined the effect of radiation and AZD3759 on cell proliferation in NSCLC cell lines expressing either wild type (WT) (H2228 and H226) or mutant EGFR (H3255 and PC-9) using MTS assay (Fig. 1a). AZD3759 alone significantly inhibited the proliferation of H3255 and PC-9 cells, with  $GI_{50}$  7.6 nM and 8.9 nM, respectively. Whereas, EGFR WT cells were insensitive to AZD3759, with  $GI_{50} > 5 \mu\text{M}$  in H226 cells and hardly any effect in H2228 cells. When AZD3759 was combined with radiation, a synergistic effect on inhibiting of cell proliferation was detected in H3255 cells treated with 10 nM AZD3759 and in PC-9 cells treated with 30 nM AZD3759 ( $CI < 1$ , Supporting Information Table S1 and Fig. S1), whereas an antagonistic effect was detected when AZD3759 at the low concentration ( $<10$  nM in H3255 cells and  $<30$  nM in PC-9 cells). In H226 and H2228 cells, there was antagonistic effect even the concentration of AZD3759 was up to 30  $\mu\text{M}$  ( $CI > 1$ , data not shown). We then further evaluated the survival of cells treated with either radiation or AZD3759 in combination with radiation by using CFA (Fig. 1b and Supporting Information Table S2). In PC-9 cells, a synergistic effect on inhibiting cell survival was detected when 10 nM AZD3759 was combined with radiation, with DEF of 1.82 ( $p < 0.0001$ , AZD3759 10 nM with radiation vs. radiation alone). In contrast, there was no synergistic effect when AZD3759 at the concentration of 5 nM ( $p = 0.383$ , AZD3759 5 nM with radiation vs. radiation alone), even a radiosensitizing effect was detected (DEF = 1.1). Similarly, there was no synergistic effect by AZD3759 and radiation in H226 cells either, even the concentration of AZD3759 was increased to higher than 100 nM. These results demonstrate that both the sensitivity to AZD3759 and the concentration of AZD3759 are essential for synergistic effect between AZD3759 and radiation.

### AZD3759 in combination with radiation delays DNA DSBs repair, increases cell cycle accumulation in G1 phase and abrogates G2/M checkpoint, and increases apoptosis

Considering DNA damage is the primary mechanisms in the tumor cell killing effect of radiation, we firstly detected the levels of DNA DSBs in cells treated with radiation and AZD3759 by measuring the mean percentage of cells with positive  $\gamma$ H2AX ( $\geq 5$  foci per cell, Fig. 2). 3 Gy radiation-induced increase in  $\gamma$ H2AX positive cells peaked at 2 hr and gradually reduced to normal level at 48 hr after radiation. AZD3759 alone produced no significant induction of  $\gamma$ H2AX foci. However, AZD3759 combined with radiation significantly increased the percentage of  $\gamma$ H2AX positive cells compared to radiation alone. Thus, AZD3759 inhibits the repair of radiation-induced DNA DSBs.

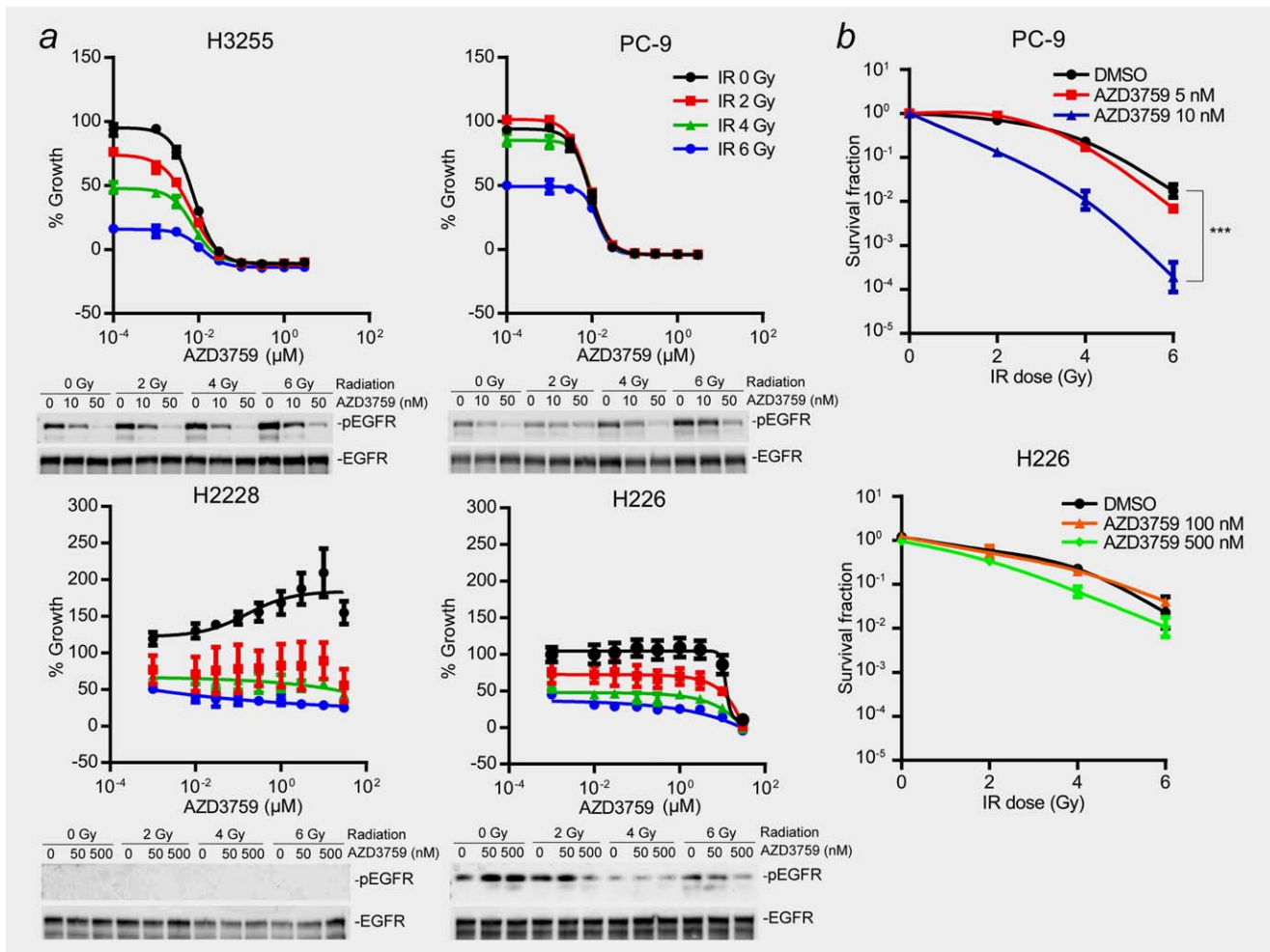


**Figure 1.** The effects of radiation and AZD3759 on cell proliferation and survival in NSCLC cell lines expressing wild-type EGFR or EGFRm. (a) Cell proliferation in MTS assay. Expression of pEGFR upon treatment with AZD3759 and/or radiation was shown in the lower part for the corresponding cell lines. (b) Cell survival in CFA. \*\*\* $p < 0.0001$  for the survival of PC-9 cells treated with radiation and 10 nM AZD3759 vs. radiation alone; linear regression. Survival curves were normalized to drug effects on plating efficiency. [Color figure can be viewed at [wileyonlinelibrary.com](http://wileyonlinelibrary.com)]

We next assessed the effect of AZD3759 and radiation on cell cycle distribution (Fig. 3a). Within 72 hr after treatment, AZD3759 dose-dependently increased the percentage of cells in G1 phase, and decreased the percentage of cells in S and G2/M phase. 15 Gy radiation markedly increased the percentage of cells in G2/M phase, and the percentage of cells in S phase was substantially increased in response to 3 Gy radiation. When AZD3759 was combined with radiation, AZD3759 significantly increased the percentage of cells in G1 phase and decreased the percentage of cells in G2/M phase, in both 3 Gy and 15 Gy radiation. Besides, AZD3759 markedly decreased the 3 Gy radiation-induced S phase accumulation, whereas the percentage of cells in S phase was slightly increased when combined with 15 Gy radiation. Conclusively, treatment with AZD3759 increases cell cycle accumulation in G1 phase and abrogates the radiation-activated G2/M checkpoint.

We also looked into sub-G1 across different time points, which is an indicator of early apoptosis (Fig. 3b). Both AZD3759 alone and radiation alone led to an increase in

apoptosis within 72 hr after treatment. AZD3759 combined with radiation markedly increased the percentage of apoptosis compared to either treatment alone at the 48-hr and 72-hr time points.

#### AZD3759 suppresses the repair of radiation-induced DNA DSBs through inhibiting the HR and NHEJ repair pathway and abrogating the G2/M checkpoint

We then evaluated the effect of radiation and AZD3759 on EGFR signaling pathway at the 2-hr time points. There was an increase in pEGFR, pAKT and pERK when cells were exposed to radiation. Administration of AZD3759 inhibited EGFR phosphorylation and downstream signaling pathways, pAKT and pERK, in spite of radiation (Fig. 4a). When we further evaluated the levels of pEGFR in cytoplasm and nucleus with/without radiation, we found a downregulation of pEGFR in both cytoplasm and nucleus in the presence of AZD3759. DNA-PKcs level was decreased in cytoplasm while had no change in nucleus (Fig. 4b). We also conducted co-IP

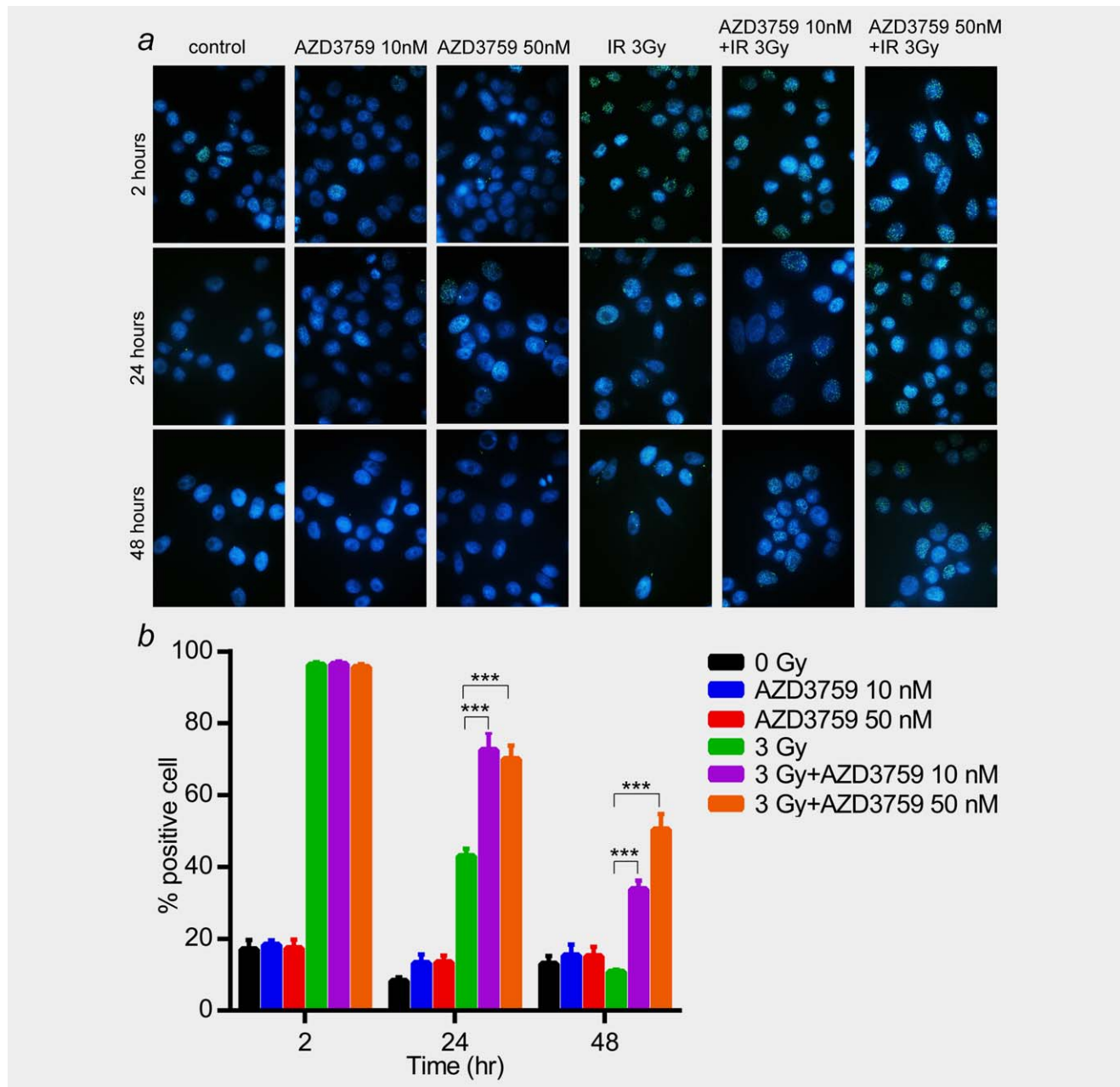


**Figure 2.** The effects of AZD3759 on radiation-induced DNA double-strand breaks (DSBs). (a) Representative IF staining of  $\gamma$ H2AX foci at 2, 24 and 48 hr after treatment in PC-9 cells. (b) Mean percentage of cells with positive  $\gamma$ H2AX in different treatment groups. Data shown in figures are mean  $\pm$  SEM, *t*-test. \*\*\**p* < 0.001 for radiation + AZD3759 vs. radiation alone. [Color figure can be viewed at [wileyonlinelibrary.com](http://wileyonlinelibrary.com)]

to evaluate the effect of radiation and AZD3759 on the expression of EGFR/DNA-PKcs complex in nucleus and cytoplasm (Fig. 4b; Supporting Information Fig. S2). We found that radiation increased the expression of EGFR/DNA-PKcs complex in nucleus while did not changed it in cytoplasm. AZD3759 increased this complex in cytoplasm. When AZD3759 was combined with radiation, the expression of EGFR/DNA-PKcs complex was decreased in nucleus while increased in cytoplasm. Thus, AZD3759 may translocate the radiation-induced EGFR/DNA-PKcs complex from nucleus to cytoplasm.

We further evaluated the expression of DNA damage response and repair (DRR) related proteins at the 24-hr and 48-hr time points (Fig. 4c). PC-9 cells exhibited high baseline rad51 expression, which is the major regulator of the homologous recombination (HR) DNA DSBs repair pathway. In response to radiation, the expression of rad51 was decreased dose-dependently 24 hr after treatment, which were back to normal level in cells treated with  $\leq 9$  Gy radiation while kept in low level in cells treated with 15 Gy radiation 48 hr after treatment. AZD3759 significantly decreased the expression of rad51 24 hr after treatment, and this inhibition effect even

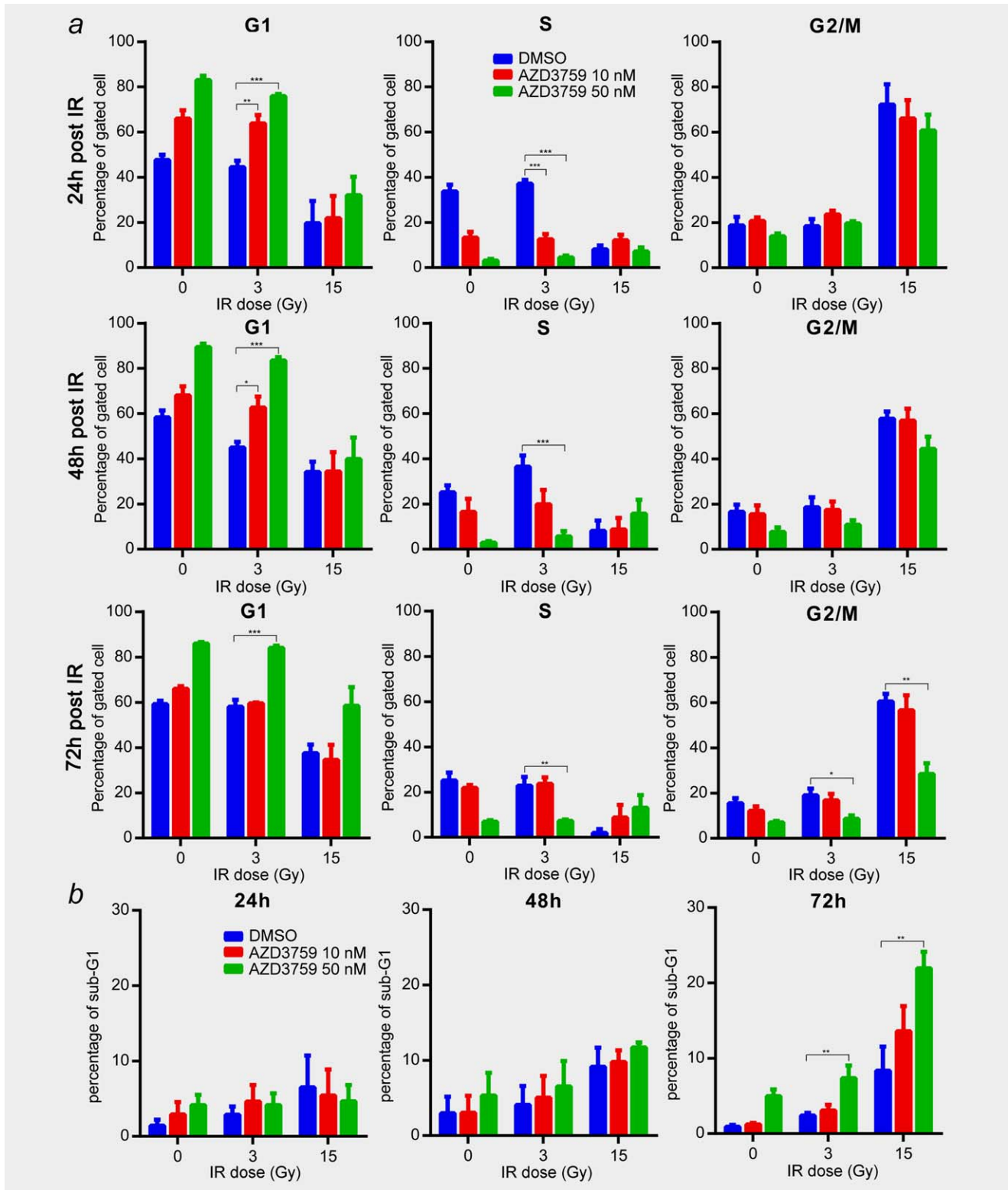
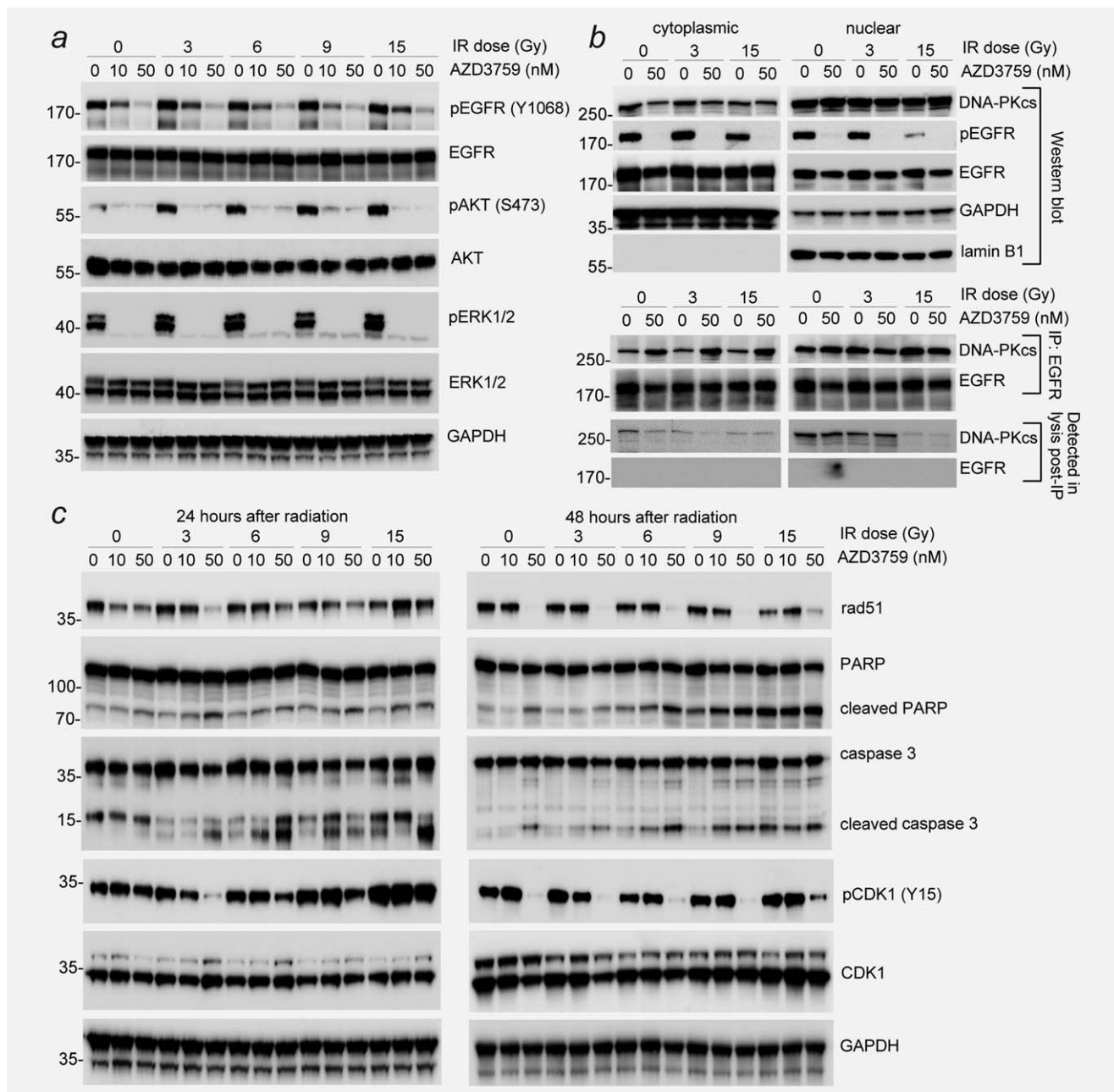


Figure 3. The effects of AZD3759 and radiation on cell cycle distribution and cell apoptosis. The percentage of cells in G1, S and G2/M phase (a) and cell apoptosis (b) in different treatment groups at the 24-hr, 48-hr and 72-hr time points. \* $p < 0.05$ , \*\* $p < 0.01$ , \*\*\* $p < 0.001$  for radiation combined with AZD3759 vs. radiation alone. [Color figure can be viewed at [wileyonlinelibrary.com](http://wileyonlinelibrary.com)]



**Figure 4.** The effects of AZD3759 and radiation on EGFR signaling pathway and DNA damage response signaling. (a) EGFR signaling pathway in different treatment groups. Cells were harvested at the 2-hr time point, whole cell proteins were analyzed by western blot for the indicated markers. (b) Interactions between EGFR and DNA-PKcs in nucleus and cytoplasm in different treatment groups. Cells were harvested at the 24-hr time point, cytoplasmic and nuclear extracts were prepared. The upper part showed the distribution of EGFR and DNA-PKcs in cytoplasm and nucleus in different treatment groups. The lower part showed the result of co-IP. Cytoplasmic and nuclear proteins were immunoprecipitated with total EGFR antibody and analyzed by western blot for the indicated proteins. (c) DNA damage response signaling in different treatment groups. Cells were harvested at the 24-hr and 48-hr time points, whole cell proteins were prepared and analyzed by western blot for the indicated markers.

more pronounced 48 hr after treatment, regardless of radiation. The expression of phosphorylated CDK1 Tyr15 was assessed, which play an important role in the regulation of G2/M checkpoint. It was found that radiation induced a dose-dependently increase in pCDK1 (Tyr15) 24 hr after treatment, which was back to normal level 48 hr after

treatment. AZD3759 alone slightly decreased it 24 hr after treatment and obviously decreased it 48 hr after treatment. When combined AZD3759 with radiation, the expression of pCDK1 (Tyr15) was significantly decreased, and this inhibition effect even more obvious at the 48-hr time points. In addition, we also detected the level of cleaved PARP and

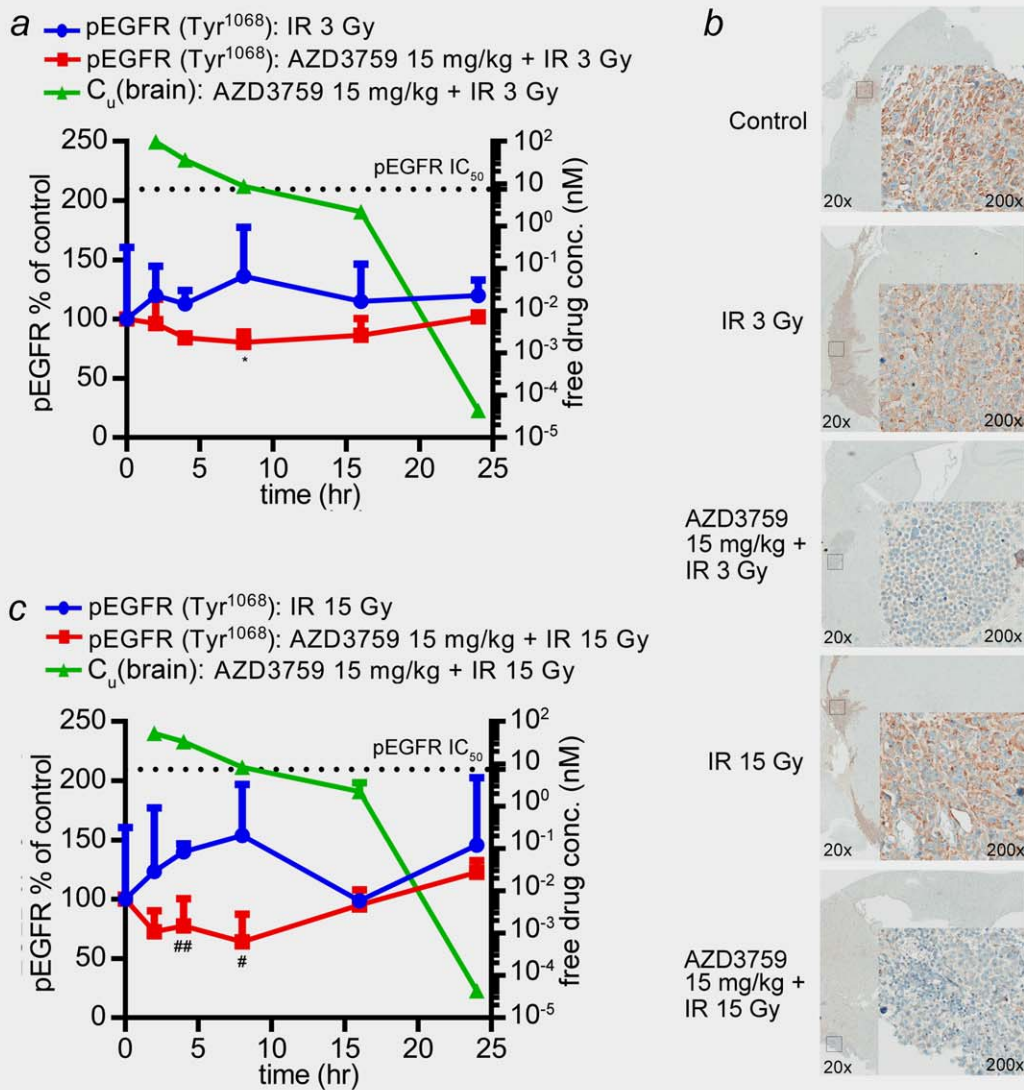


**Figure 5.** PK and PD correlations in PC-9 BM models treated with radiation and AZD3759. The level of pEGFR and the free concentration of AZD3759 in brain after treated with radiation and AZD3759 were shown in *a* (3 Gy radiation) and *b* (15 Gy radiation). The pEGFR IC<sub>50</sub> of PC-9 cells was 7.4 nM. \**p* = 0.016, AZD3759 combined with 3 Gy radiation vs. 3 Gy radiation alone 4 hr after radiation. #*p* = 0.031 and ##*p* = 0.009 for AZD3759 combined with 15 Gy radiation vs. 15 Gy radiation alone 8 hr and 4 hr after radiation, respectively. (c) Representative images of pEGFR in the brain tumor tissues 8 hr after AZD3759 dosing. C<sub>u</sub>(brain), free concentration of AZD3759 in brain. [Color figure can be viewed at [wileyonlinelibrary.com](http://wileyonlinelibrary.com)]

cleaved caspase 3 (CC3), which are cell apoptosis indicators. In line with the results of sub-G1 analysis, combination therapy with AZD3759 and radiation markedly increased cell apoptosis compared to individual treatment.

#### AZD3759 displays high distribution in mice brain and inhibits the expression of pEGFR in BM models

To determine whether or not cranial radiation influence the BBB penetration of AZD3759, we compared the  $K_{p,brain}$  and  $K_{puu,brain}$  between mice treated with AZD3759 alone and mice treated with AZD3759 combined with radiation within 24 hr after treatment (Supporting Information Table S3). The results showed instead of increasing the BBB penetration

of AZD3759, radiation decreased the BBB penetration of AZD3759 within 24 hr after treatment, with the  $K_{p,brain}$  and  $K_{puu,brain}$  were 2.81 and 0.64, 1.86 and 0.42, 1.55 and 0.35 in mice treated with AZD3759 alone, AZD3759 combined with 3 Gy radiation, and AZD3759 combined with 15 Gy radiation, respectively. However, the free concentration of AZD3759 kept at a high level in brain when combined with radiation, with the free concentration of AZD3759 in brain was above the pEGFR IC<sub>50</sub> of PC-9 cells for about 8 hr (Fig. 5).

We then assessed the activity of AZD3759 in brain by detecting the extent and duration of pEGFR reduction in mice treated with AZD3759 and radiation relative to mice treated with radiation alone (Fig. 5). 3 Gy and 15 Gy

radiation-induced increase in pEGFR expression in brain tumor peaked at 7 hr and declined to normal level at 23 hr after radiation. When treated with AZD3759 and radiation, AZD3759 inhibited both the basal expression and radiation-induced expression of pEGFR. Collectively, these results validate the great CNS penetration and the potent activity of AZD3759 in BM in the context of radiation.

#### **AZD3759 combined with radiation enhances the antitumor efficacy in BM models**

To evaluate whether the enhanced efficacy of AZD3759 combined with radiation observed *in vitro* could be translated into an *in vivo* tumor model, we assessed the antitumor efficacy of this combination therapy in BM models in nude mice. For animal welfare, the *in vivo* efficacy study was ended 100 days after treatment start. As shown in Figure 6a, AZD3759 alone significantly inhibited tumor growth. The antitumor activity of AZD3759 alone was much better than radiation alone. As expected, combination therapy with AZD3759 and radiation was more effective than individual treatment, and body weight loss in animals treated with combination therapy did not exceed 20% (Fig. 6b). We also compared tumor areas in different treatment groups at the end of our study (Day 100). Combination therapy significantly decreased tumor area in brain compared to either treatment alone (Fig. 6c). Besides, no significant difference in antitumor activity was detected between radiation concurrently with AZD3759 and radiation sequentially with AZD3759. These data indicate that combination therapy with AZD3759 and radiation enhanced the antitumor activity in BM compared to single treatment.

#### **AZD3759 increases the radiation-induced apoptosis and inhibits cell proliferation in BM models**

We also tested the expression of molecular markers for cell proliferation (Ki-67) and apoptosis (CC3) in tumor tissues in different treatment groups using IHC assay (Supporting Information Fig. S3). Our data showed that radiation alone slightly increased the positive staining of CC3. Combined AZD3759 with radiation significantly increased the positive staining of CC3. Radiation treatment increased the expression of Ki-67 at 3 hr and back to normal level 8 hr after radiation. Combined AZD3759 with radiation significantly inhibited both the radiation-induced expression and basal level expression of Ki-67. Thus, in consistent with *in vitro* results, AZD3759 increases radiation-induced cell apoptosis and inhibits cell proliferation in tumor bearing mice.

#### **Discussion**

In our study, we evaluated the effect of AZD3759 in combination with radiation in both *in vitro* and *in vivo*. In EGFRm cell lines, H3255 and PC-9, AZD3759 enhanced the inhibitory effect of radiation on cell proliferation and cell survival. Whereas this effect was not observed in the EGFR WT cell lines, H2228 and H226, even though the H2228 cell was sensitive to radiation. This suggests that a sensitivity to EGFR-

TKIs is essential to achieve enhanced efficacy when combined with radiation. This is in line with previous studies.<sup>12</sup> Moreover, our results showed that the synergistic effect was detected only when radiation was combined with a relative high concentration of AZD3759, thus the concentration of AZD3759 may be another factor determine the enhanced efficacy of radiation combined with AZD3759. This could partially explain the different response when first-generation EGFR-TKIs and radiation was used for intracranial lesions compared to these in extracranial lesions.

Mechanisms underlying the radiosensitizing effect of EGFR-TKIs have been well defined, which is involved in suppressing cell proliferation and survival, inducing apoptosis, and inhibiting DNA damage repair. Our data did validate it. Besides, we also detected the detailed mechanisms for inhibiting effect of EGFR-TKIs on DNA damage repair. The results of our data showed that combined AZD3759 with radiation significantly prolonged the presence of DNA DSBs compared to radiation alone, this is in line with previous studies.<sup>13,27,28</sup> Moreover, the results of western blot and co-IP showed that in response to radiation, there was radiation dose-dependently decrease in rad51 expression and dose-dependently increase in binding between DNA-PKcs and EGFR in nucleus. This suggests that in response to radiation, the role of HR is weakened while the role of NHEJ is enhanced. However, AZD3759 decreased both the expression of rad51 and the binding between DNA-PKcs and EGFR in nucleus, regardless of treatment alone or combined with radiation. Thus, mechanisms underlying the inhibitory effect of AZD3759 on DNA DSBs repair involved in inhibiting both the HR and NHEJ repair pathway.

In response to radiation, tumor cells activate the G2/M checkpoint to assist DNA damage repair.<sup>29,30</sup> AZD3759 dose-dependently decreased the percentage of cells in G2/M phase, regardless of treatment alone or combined with radiation. Combined with the results of western blot that AZD3759 inhibited the expression of pCDK1 (Tyr15), these results suggest that AZD3759 abrogate the G2/M checkpoint, thus shorten time for DNA damage repair. Collectively, the inhibitory effect of AZD3759 on DNA DSBs repair also involved in G2/M checkpoint abrogation. The increased apoptosis showed in sub-G1, cleaved caspase 3 and cleaved PARP further confirm the persistent DNA DSBs that induced by radiation and AZD3759.

Aside from the potential radiosensitizing effect of EGFR-TKIs, another rationale for combining EGFR-TKIs with radiation is radiation might enhance the BBB penetration of EGFR-TKIs. Preclinical studies showed cranial radiation increased the permeability of BBB 90 days after radiation, while no significant change in permeability was detected at an early stage.<sup>31</sup> Besides, two self-controlled clinical studies showed that WBRT did not significantly increase the penetration of gefitinib or icotinib within 30 days after radiation.<sup>32,33</sup> In our study, instead of increasing the penetration of AZD3759 through BBB, radiation decreased the penetration of AZD3759 through BBB within 24 hr. Thus, the role of

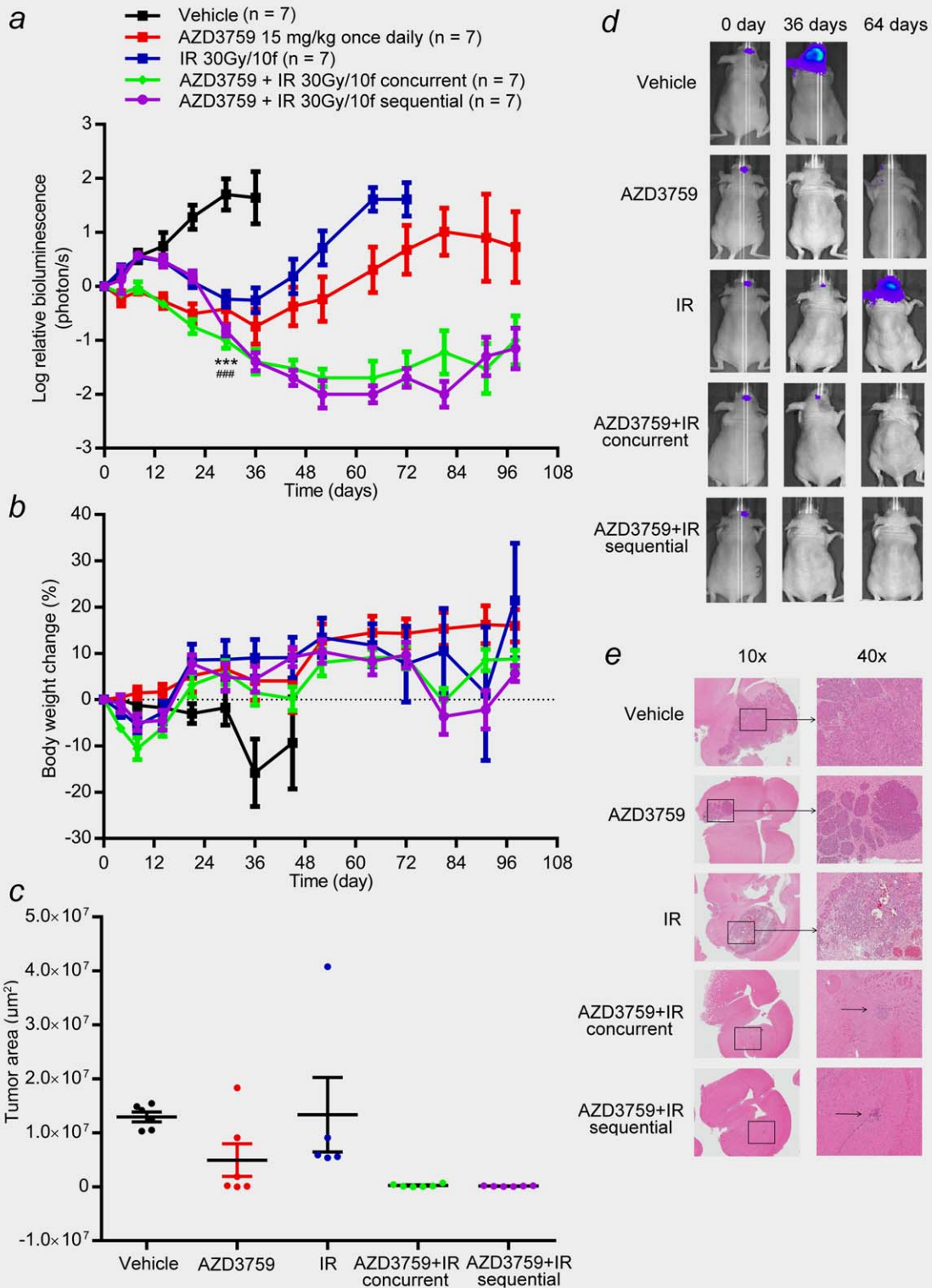


**Figure 6.** Anti-tumor activity of AZD3759 combined with radiation in the PC-9 BM models in nude mice. (a) Luciferin signals in different treatment groups. At Day 29 after starting treatment,  $***p < 0.0001$  for radiation combined with AZD3759 vs. radiation alone;  $###p < 0.0001$  for radiation combined with AZD3759 vs. AZD3759 alone; two-way ANOVA. (b) Body weight (BW) change in different treatment groups. (c) Tumor areas at the end of *in vivo* efficacy study in different treatment groups. (d) Representative images of luciferin signals at indicated days after starting treatment. (e) Representative images of tumor area at the end of *in vivo* efficacy study. [Color figure can be viewed at [wileyonlinelibrary.com](http://wileyonlinelibrary.com)]

cranial radiation in increasing the BBB penetration of EGFR-TKIs might be minor and unreliable. However, the great BBB penetration of AZD3759 ensures the brain concentration of AZD3759 is high enough, thus AZD3759 function its radiosensitizing effect well in brain when combined with radiotherapy.

Clinically, the optimal treatment modality and treatment sequence for BM from EGFR-mutant NSCLC is unclear. With evidence showed that EGFR-TKIs monotherapy, especially the novel agents AZD3759 and osimertinib which displayed promising BBB penetration, demonstrated satisfactory intracranial control,<sup>7,34,35</sup> and there were study reported that icotinib was associated with significantly longer intracranial control than WBRT.<sup>36</sup> Besides, a retrospective study demonstrated that the addition of WBRT did not further improved the efficacy of EGFR-TKIs.<sup>37</sup> These evidences trigger debates about the role of radiotherapy in the treatment of BM from EGFR-mutant NSCLC, would EGFR-TKIs replace radiotherapy as first line therapy? When is the optimal timing to perform radiotherapy, combined with EGFR-TKIs as first line therapy or as salvage therapy when intracranial disease progressed from EGFR-TKIs? Our study provides preclinical data for it. In our study, AZD3759 monotherapy displayed potent antitumor efficacy in EGFR-mutant BM model, which were significantly better than the standard regimen for WBRT (30 Gy/10f). Combination therapy with AZD3759 and radiation was more effective than individual treatment. These results indicate that radiation is irreplaceable in the treatment of BM from EGFR-mutant NSCLC, even in the era of EGFR-TKIs with high BBB penetration, such as AZD3759 and osimertinib. EGFR-TKIs combined with radiotherapy might be a better first line treatment option for BM from EGFR-mutant NSCLC. Moreover, our study showed that the antitumor activity in combination therapy displayed no difference between radiation concurrently with AZD3759 and radiation sequentially with AZD3759, thus, delayed intervention of AZD3759 might be possible in the first-line treatment of BM,

especially for patients who are not tolerable to concurrent treatment.

We also measured the body weight change of mice during the *in vivo* efficacy study to investigate the treatment-related adverse effect. The results showed that body weight loss did not exceed 20% in animals treated with AZD3759/radiation alone or AZD3759 combined with radiation. No animals stopped treatment for severe adverse effect. Thus, toxicity of AZD3759 combined with radiation is well tolerable. Detection of neurocognitive function need more specialized methods, and there were still no normalized standards to define cognitive impairment in mice. Thus, we have not measured the neurocognitive function.

There were still several limitations in our study. First, the *in vivo* efficacy study was conducted in nude mice, which might neglect the role of host immunity in the antitumor activity of radiation and AZD3759. As it has been well established that the notable therapeutic effect of high-dose single fraction radiation is partly rely on the antitumor immunity.<sup>38</sup> While it remains unclear about the effect of EGFR-TKIs combined with or without radiation on host antitumor immunity, and our further studies are ongoing to clarify the immune modulating effect of EGFR-TKIs and radiation. Second, our study did not evaluate the neurotoxicity of combination therapy, especially the radiation-related impairment of cognitive function. However, body weight change was measured during the *in vivo* efficacy study, and the results showed adverse effect of AZD3759 combined with radiation was well tolerable. Nevertheless, the results of our study did provide theoretical basis for further clinical studies.

### Acknowledgements

We thank Shuqiong Fan for her work on sample preparation of tumor-bearing brain tissues for IHC assay, thank Kunji Liu for his work on providing cells for *in vivo* BM model. We would also thank Lingli Zhang for her work on *in vivo* DMPK assay.

### References

- Barnholtz-Sloan JS, Sloan AE, Davis FG, et al. Incidence proportions of brain metastases in patients diagnosed (1973 to 2001) in the Metropolitan Detroit Cancer Surveillance System. *JCO* 2004;22:2865–72.
- Shin DY, Na II, Kim CH, et al. EGFR mutation and brain metastasis in pulmonary adenocarcinomas. *J Thorac Oncol* 2014;9:195–9.
- Rangachari D, Yamaguchi N, VanderLaan PA, et al. Brain metastases in patients with EGFR-mutated or ALK-rearranged non-small-cell lung cancers. *Lung Cancer* 2015;88:108–11.
- Patchell RA. The management of brain metastases. *Cancer Treat Rev* 2003;29:533–40.
- Sperduto PW, Kased N, Roberge D, et al. Summary report on the graded prognostic assessment: an accurate and facile diagnosis-specific tool to estimate survival for patients with brain metastases. *JCO* 2012;30:419–25.
- Andrews DW, Scott CB, Sperduto PW, et al. Whole brain radiation therapy with or without stereotactic radiosurgery boost for patients with one to three brain metastases: phase III results of the RTOG 9508 randomised trial. *Lancet* 2004; 363:1665–72.
- Iuchi T, Shingyoji M, Sakaida T, et al. Phase II trial of gefitinib alone without radiation therapy for Japanese patients with brain metastases from EGFR-mutant lung adenocarcinoma. *Lung Cancer* 2013;82:282–7.
- Park SJ, Kim HT, Lee DH, et al. Efficacy of epidermal growth factor receptor tyrosine kinase inhibitors for brain metastasis in non-small cell lung cancer patients harboring either exon 19 or 21 mutation. *Lung Cancer* 2012;77:556–60.
- Lee SM, Lewanski CR, Counsell N, et al. Randomized trial of erlotinib plus whole-brain radiotherapy for NSCLC patients with multiple brain metastases. *J Natl Cancer Inst* 2014;106:pii: dju151. PMID: 25031274.
- Welsh JW, Komaki R, Amini A, et al. Phase II trial of erlotinib plus concurrent whole-brain radiation therapy for patients with brain metastases from non-small-cell lung cancer. *JCO* 2013;31: 895–902.
- Sperduto PW, Wang M, Robins HI, et al. A phase 3 trial of whole brain radiation therapy and stereotactic radiosurgery alone versus WBRT and SRS with temozolomide or erlotinib for non-small cell lung cancer and 1 to 3 brain metastases: Radiation Therapy Oncology Group 0320. *Int J Radiat Oncol Biol Phys* 2013;85:1312–8.
- Bokobza SM, Jiang Y, Weber AM, et al. Short-course treatment with gefitinib enhances curative potential of radiation therapy in a mouse model of human non-small cell lung cancer. *Int J Radiat Oncol Biol Phys* 2014;88:947–54.

13. Tanaka T, Munshi A, Brooks C, et al. Gefitinib radiosensitizes non-small cell lung cancer cells by suppressing cellular DNA repair capacity. *Clin Cancer Res* 2008;14:1266–73.
14. Chinnaiyan P, Huang S, Vallabhaneni G, et al. Mechanisms of enhanced radiation response following epidermal growth factor receptor signaling inhibition by erlotinib (Tarceva). *Cancer Res* 2005;65:3328–35.
15. Komaki R, Allen PK, Wei X, et al. Adding erlotinib to chemoradiation improves overall survival but not progression-free survival in stage III non-small cell lung cancer. *Int J Radiat Oncol Biol Phys* 2015;92:317–24.
16. Lilienbaum R, Samuels M, Wang X, et al. A phase II study of induction chemotherapy followed by thoracic radiotherapy and erlotinib in poor-risk stage III non-small-cell lung cancer: results of CALGB 30605 (Alliance)/RTOG 0972 (NRG). *J Thorac Oncol* 2015;10:143–7.
17. Zeng Q, Wang J, Cheng Z, et al. Discovery and evaluation of clinical candidate AZD3759, a potent, oral active, central nervous system-penetrant, epidermal growth factor receptor tyrosine kinase inhibitor. *J Med Chem* 2015;58:8200–15.
18. Yang Z, Guo Q, Wang Y, et al. AZD3759, a BBB-penetrating EGFR inhibitor for the treatment of EGFR mutant NSCLC with CNS metastases. *Sci Transl Med* 2016;8:368ra172. PMID: 27928026.
19. Zhang S, Zheng X, Huang H, et al. Afatinib increases sensitivity to radiation in non-small cell lung cancer cells with acquired EGFR T790M mutation. *Oncotarget* 2015;6:5832–45.
20. Chou TC. Drug combination studies and their synergy quantification using the Chou–Talalay method. *Cancer Res* 2010;70:440–6.
21. Franken NA, Rodermond HM, Stap J, et al. Clonogenic assay of cells *in vitro*. *Nat Protoc* 2006;1:2315–9.
22. Lobrich M, Shibata A, Beucher A, et al. gamma-H2AX foci analysis for monitoring DNA double-strand break repair: strengths, limitations and optimization. *Cell Cycle* 2010;9:662–9.
23. Martin NT, Nahas SA, Tunuguntla R, et al. Assessing 'radiosensitivity' with kinetic profiles of gamma-H2AX, 53BP1 and BRCA1 foci. *Radiother Oncol* 2011;101:35–8.
24. Lal S, Lacroix M, Tofilon P, et al. An implantable guide-screw system for brain tumor studies in small animals. *J Neurosurg* 2000;92:326–33.
25. Ballard P, Yates JW, Yang Z, et al. Preclinical comparison of osimertinib with other EGFR-TKIs in EGFR-mutant NSCLC brain metastases models, and early evidence of clinical brain metastases activity. *Clin Cancer Res* 2016;22:5130–40.
26. Yates JW, Ashton S, Cross D, et al. Irreversible inhibition of EGFR: modeling the combined pharmacokinetic–pharmacodynamic relationship of osimertinib and its active metabolite AZ5104. *Mol Cancer Ther* 2016;15:2378–87.
27. Kang KB, Zhu C, Wong YL, et al. Gefitinib radiosensitizes stem-like glioma cells: inhibition of epidermal growth factor receptor–Akt–DNA–PK signaling, accompanied by inhibition of DNA double-strand break repair. *Int J Radiat Oncol Biol Phys* 2012;83:e43–e52.
28. Cuneo KC, Nyati MK, Ray D, et al. EGFR targeted therapies and radiation: optimizing efficacy by appropriate drug scheduling and patient selection. *Pharmacol Ther* 2015;154:67–77.
29. Santivasi WL, Xia F. Ionizing radiation-induced DNA damage, response, and repair. *Antioxid Redox Signal* 2014;21:251–9.
30. Rhind N, Russell P. Signaling pathways that regulate cell division. *Cold Spring Harb Perspect Biol* 2012;4:a005942. pii:a005942. PMID: 23028116.
31. Yuan H, Gaber MW, Boyd K, et al. Effects of fractionated radiation on the brain vasculature in a murine model: blood–brain barrier permeability, astrocyte proliferation, and ultrastructural changes. *Int J Radiat Oncol Biol Phys* 2006;66:860–6.
32. Zhou L, He J, Xiong W, et al. Impact of whole brain radiation therapy on CSF penetration ability of icotinib in EGFR-mutated non-small cell lung cancer patients with brain metastases: results of phase I dose-escalation study. *Lung Cancer* 2016;96:93–100.
33. Fang L, Sun X, Song Y, et al. Whole-brain radiation fails to boost intracerebral gefitinib concentration in patients with brain metastatic non-small cell lung cancer: a self-controlled, pilot study. *Cancer Chemother Pharmacol* 2015;76:873–7.
34. Ahn MJ, Kim DW, Cho BC, et al. Activity and safety of AZD3759 in EGFR-mutant non-small-cell lung cancer with CNS metastases (BLOOM): a phase 1, open-label, dose-escalation and dose-expansion study. *Lancet Respir Med* 2017;5:891–902.
35. Yang JC-H, Cho BC, Kim D-W, et al. Osimertinib for patients (pts) with leptomeningeal metastases (LM) from EGFR-mutant non-small cell lung cancer (NSCLC): updated results from the BLOOM study. ASCO, 2017. [http://ascopubs.org/doi/abs/10.1200/JCO.2017.35.15\\_suppl.2020](http://ascopubs.org/doi/abs/10.1200/JCO.2017.35.15_suppl.2020).
36. Yang JJ, Zhou C, Huang Y, et al. Icotinib versus whole-brain irradiation in patients with EGFR-mutant non-small-cell lung cancer and multiple brain metastases (BRAIN): a multicentre, phase 3, open-label, parallel, randomised controlled trial. *Lancet Respir Med* 2017;5:707–16.
37. Jiang T, Su C, Li X, et al. EGFR TKIs plus WBRT demonstrated no survival benefit other than that of TKIs alone in patients with NSCLC and EGFR mutation and brain metastases. *J Thorac Oncol* 2016;11:1718–28.
38. Burnette BC, Liang H, Lee Y, et al. The efficacy of radiotherapy relies upon induction of type I interferon-dependent innate and adaptive immunity. *Cancer Res* 2011;71:2488–96.